Electron field emission from carbon nanotubes on porous alumina

D. Lysenkov, H. Abbas, and G. Müller[a)]
FB C Physik, Bergische Universität Wuppertal, D-42097 Wuppertal, Germany

J. Engstler, K. P. Budna,[b)] and J. J. Schneider
FB Chemie, Eduard-Zintl-Institut, TU Darmstadt, D-64287 Darmstadt, Germany

(Received 24 September 2004; accepted 10 January 2005; published 7 April 2005)

We have synthesized carbon nanotubes by chemical vapor deposition using ferrocene as single source organometallic precursor both on commercial (Anodisc®) and electrochemically etched porous alumina templates. Carbon nanotubes of about 20 nm diameter and some μm in length appeared apart on the alumina membranes. Integral field emission measurements of these cathodes were performed in a diode configuration with luminescent screen. High emitter number densities of at least $10\,000/\mathrm{cm}^2$ and current densities up to $32\ \mathrm{mA/cm}^2$ were obtained at an electric field of $7.2\ \mathrm{V}/\mu\mathrm{m}$. Cathode processing at pressures in the range from 10^{-7} to 5×10^{-4} mbar resulted in improved current stability measured over 18 h. High resolution emitter distributions obtained with the field emission scanning microscope yielded up to $62\,000$ emitters/cm^2 at $23\ \mathrm{V}/\mu\mathrm{m}$. Single emitter investigations showed Fowler–Nordheim behavior up to 1 μA and current limits up to 12 μA in dc operation. Reversible switching between different emission states was also observed. Possible explanations of these phenomena and their impact for applications will be discussed. [DOI: 10.1116/1.1868696]

I. INTRODUCTION

Recent investigations on cold cathodes are focusing on carbon nanotubes (CNTs) because of their simple fabrication techniques and unique field emission (FE) properties which are well suited for vacuum nanoelectronic devices. Applications like intense light[1] and pulsed x-ray sources[2] require that CNTs provide stable and high emission currents at low electric fields and pressure levels in the high vacuum regime with long device lifetimes. While most CNT cathodes have given nA currents already at electric fields of some $\mathrm{V}/\mu\mathrm{m}$, current densities above $\mathrm{mA/cm}^2$ are rarely reported despite measured current limits up to 2 μA for single wall[3] and 20 μA for multiwall CNTs.[4] While densely populated CNT cathodes suppress FE at low fields due to mutual shielding effects,[5] separately grown CNTs with high number densities and homogeneous FE properties are difficult to achieve.[6] Moreover, CNT emitters have often shown short-term current fluctuations and long-term current degradation[7] probably due to adsorbate or heating effects. Alignment, shortening, and disruption of CNTs under high electric fields have also been observed.[8–10]

Actually, lithographic patterning of catalyst on Si substrates for nucleation[11] and chemical vapor deposition (CVD) with hydrocarbons for CNT growth are the preferred fabrication techniques for FE cathodes. The resulting arrays of free-standing CNTs, however, still show remaining nonuniformity, FE inhomogeneity, and current instabilities due to their unprotected exposure to the environment. Therefore, we have chosen another approach based on porous alumina substrates and a single-step CVD process with ferrocene as precursor which combines CNT nucleation and growth.[12] Porous alumina has proven to improve the adhesion and current limits of CNT emitters.[13] Moreover, the embedding of CNTs in lithographically defined pores of alumina membranes might be well suited to unify the field enhancement of CNT arrays and protect them against environmental influences.

In this article we report on the pressure dependence and long-term current stability of cathodes with arbitrary but separately grown CNTs on the surface of porous alumina membranes. Results on the number density of the emitters as a function of the electric field by luminescent screen imaging and on their microscopically scanned FE properties will be given. Current fluctuation and switching effects obtained by the signal analysis of single emitters will also be discussed.

II. SAMPLE PREPARATION AND MEASUREMENT TECHNIQUES

We have synthesized CNTs by CVD using ferrocene as single source precursor both on commercial (Anodisc®) and electrochemically etched porous alumina membranes (EPAM)[12] of different thickness (60/200 μm for Anodisc®/EPAM) and pore diameter (200/50 nm for Anodisc®/EPAM). The pores of both types of membranes were partially clogged by aluminum oxide clusters prior to CNT growth. Two formation processes occur during CVD: growth of tubular structures within the pores and of CNTs on the surface of the membranes. Scanning electron microscopy, transmission electron microscopy, electron energy loss spectra, and atomic force microscopy investigations showed that the tubular structures in the pores are composed of pyrolytic carbon in which nanoscaled metallic particles are incorporated, while pure multiwall CNTs of about 20 nm diameter appear apart on the alumina surface.[14] The CNTs on Ano-

a)Author to whom correspondence should be addressed; electronic mail: mueller@venus.physik.uni-wuppertal.de
b)Present address: Institut fur Metallkunde und Werkstoffprüfung, Montan-Universität, Franz-Josef-Strasse 18, A-8700 Leoben, Germany.

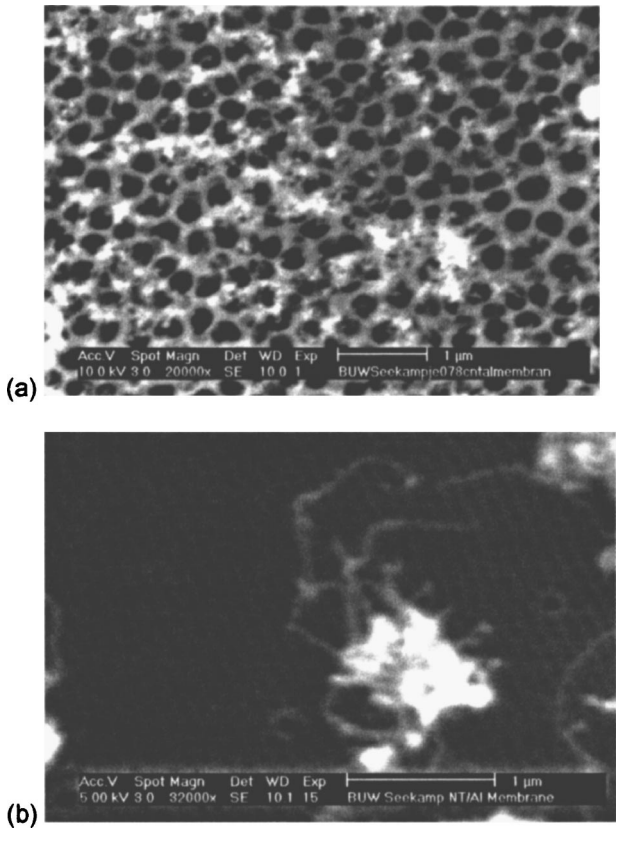

FIG. 1. SEM images of differently prepared CNT samples on: (a) Anodisc® and (b) EPAM. The white clusters on the surface consist of alumina.

disc® are short ($<\mu$m) and originate mostly from the pores, whereas the CNTs on EPAM are typically longer ($>\mu$m) and fixed to alumina clusters (see Fig. 1). Moreover, the latter CNT samples were less brittle due to the smaller pore size and larger thickness of the alumina.

Integral FE measurements of the CNT cathodes were performed up to 3 kV in a diode configuration with luminescent screen (IMLS). As shown in Fig. 2, this system with z adjustment by stepping motor and tilt correction ($\Delta z < 10$ μm) avoids a central spacer and thus prevents discharges caused by surface currents or gas desorption. For typical electrode spacings of some hundred μm, it provides the best pressure control at the sample, which can be adjusted between 10^{-7} (base) and 10^{-3} mbar (gas inlet). By means of a charge coupled device camera and some lenses an image resolution of 20 μm can be achieved. Alternatively, 10 Hz online videos of the emission evolution with two times less resolution can be recorded. Fast image analysis is provided by a digital data acquisition system and software package (ANALYSIS®). The FE uniformity was further investigated by high resolution voltage and current scans with the field emission scanning microscope (FESM) inside in an ultrahigh vacuum chamber at a pressure of about 10^{-9} mbar as described in Ref. 13. Local current–voltage ($I-V$) measurements provided electric field calibration and Fowler–Nordheim curves in the nA range. Emission current fluctuations were measured with a signal analyzer (HP25670A). The temporal resolution of about 1 ms was given by the capacity of the test setup.

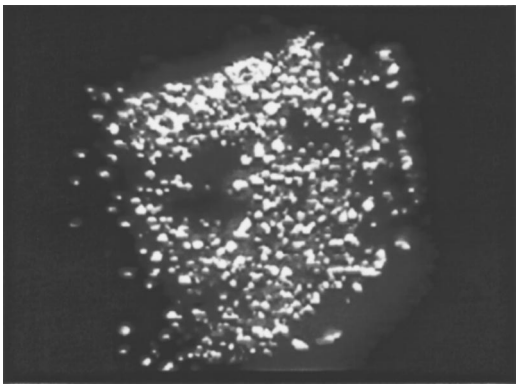

FIG. 3. IMLS image of a 28 mm^2 CNT on EPAM sample at about 4 V/μm.

III. FE RESULTS AND DISCUSSION

At first, the emission strength and uniformity of all CNT cathodes were measured with the IMLS. After some initial conditioning of enhanced edge emission,[14] reproducible images with plenty of emitters distributed over the whole sample surface were obtained. A typical image of a nearly rectangular CNT sample on EPAM at an electric field of 7.2 V/μm is shown in Fig. 3. About 360 light spots have been counted by means of the image analysis software on an

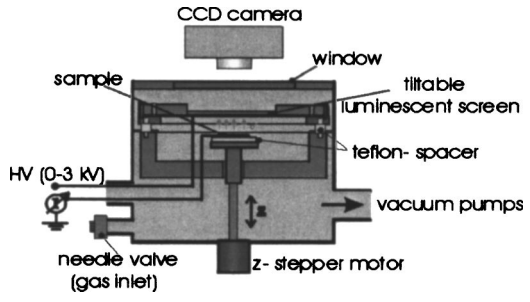

FIG. 2. Schematic of the integral $I-V$ measurement system with luminescent screen (IMLS). The gap between the cathode sample and the luminescent screen anode is adjustable by the z motor.

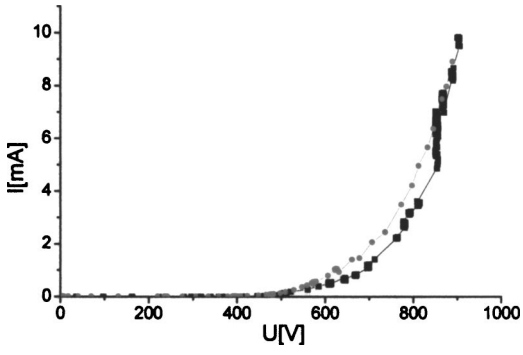

FIG. 4. Integrally measured current of the same sample as in Fig. 3 for increasing (black squares) and decreasing voltage (red circles). The electrode spacing was 125 μm.

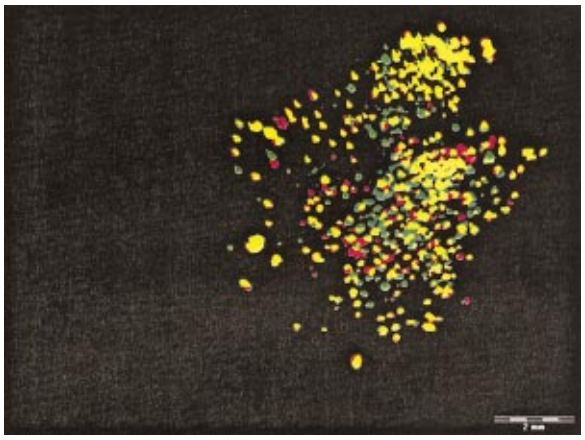

FIG. 5. Software analysis of IMLS images showing current processing effects on the same sample as in Fig. 3. The emitter distibution has partially changed after 10 min processing time, resulting in stable (yellow), activated (green) and deactivated emitters (red).

area of 28 mm^2, resulting in an emitter number density of about 10 000/cm^2. During the first increase of the voltage, processing of some emitters has often been observed which leads to small permanent current jumps in the integrally measured $I-V$ curve (Fig. 4). Beside the flickering of some light spots, i.e., their repeated on and off switching within about seconds, a permanent activation or deactivation of emitters has also been seen in the IMLS videos. The current processing effects on that sample have been revealed by means of software image analysis as shown in Fig. 5, where short-term fluctuations have been suppressed by image averaging over 5 s. After a processing time of 10 min, 54% of the emitters have remained stable, while 29% (17%) have been activated (deactivated). Soft current processing resulted in a maximum cathode current of 9 mA at 900 V, which corresponds to a high dc current density of 32 mA/cm^2. This record value for our samples was limited by a discharge rather due to phosphor evaporation from the highly illuminated screen than by the destruction of the CNTs, since traces of phosphor components (P, S, Zn) have been found on the sample after discharge.

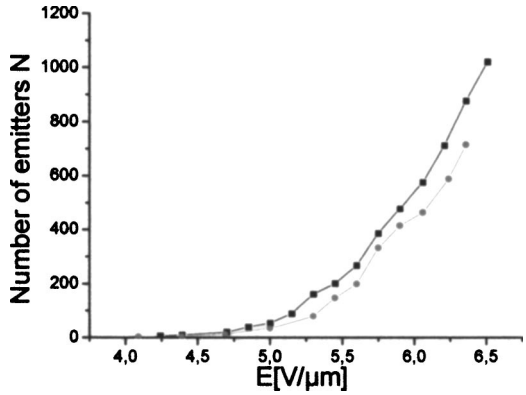

FIG. 6. Number of emitters found in IMLS images versus electric field for a 20 mm^2 CNT on EPAM sample at 10^{-6} mbar before (black squares) and after (red circles) pressure conditioning.

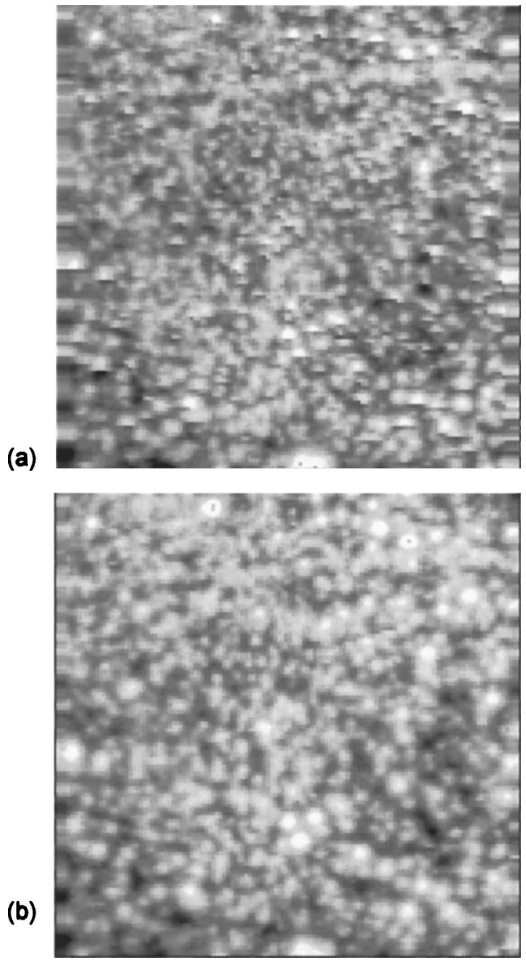

FIG. 7. FESM voltage maps between 200 V (bright) and 900 V (dark spots) correlated to fields between 5 and 23 V/μm required for 10 nA local ($\varnothing$ 5 μm) current of the same 1 mm^2 area of a CNT sample on EPAM during the: (a) first and (b) second scan. While the resulting emitter number density has been reduced from 62 000/cm^2 to 45 000/cm^2, most emitters have become stronger.

In comparison, the CNTs on Anodisc® provided similar IMLS images and emitter number densities at lower turn-on fields (about 7000/cm^2 at 3 V/μm) but with less current carrying capability ($<$6 mA/cm^2).[13] Moreover, these CNT emitters were less stable at high currents, i.e., the IMLS images revealed more permanent changes of the emitter distribution. For example, after 2 h of current processing at 250 μA the total number of emitters at a given field increased about a factor of 3. Nevertheless, the final integral $I-V$ curves were quite reproducible. Permanent alignment and desorption of gases are most often discussed as the origin of CNT emitter activation, while shortening and disruption of CNTs and adsorption of gases might cause deactivation. In order to distinguish these effects, we have tested a CNT sample on EPAM before and after a 30 min exposure to a pressure of 2×10^{-3} mbar. The change of the emitter numbers as function of the applied field resulting from IMLS image analysis is given in Fig. 6. Obviously there is some reduction of about 25%, which suggests a significant influence of adsorbates on the FE strength of CNT emitters.

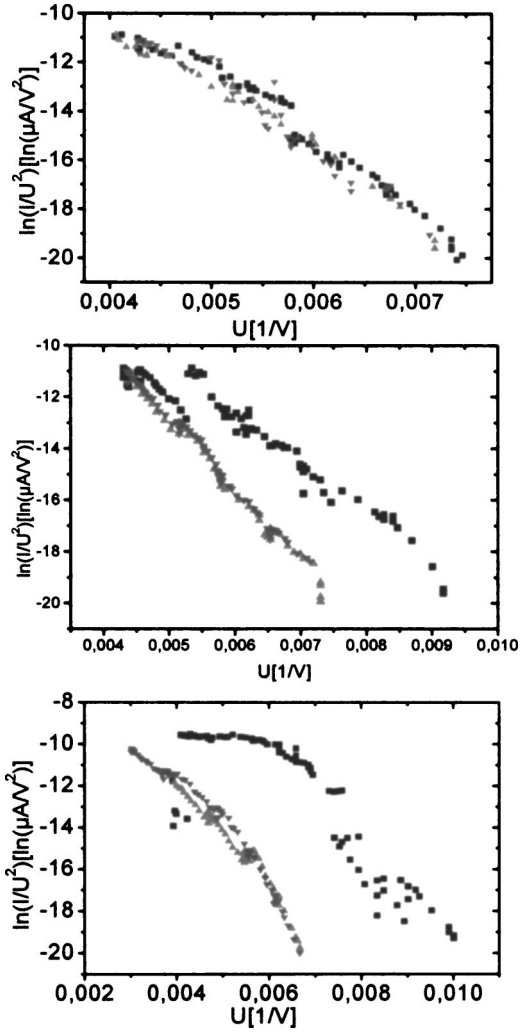

FIG. 8. Locally measured FN plots for three emitters of a CNT sample on EPAM for consecutive cycles showing: (a) nearly reversible current, (b) degradation, and (c) saturation effects during first rise (black squares), fall (red triangles), and second rise of current (blue triangles).

High resolution emitter distributions obtained by current scans with the FESM provided slightly higher number densities than the IMLS results as expected. Moreover, the potential number of CNT emitters at high electric fields was determined by voltage scans to be about $24\,000/\mathrm{cm}^2$ at $12\ \mathrm{V}/\mu\mathrm{m}$ for Anodisc® and $62\,000/\mathrm{cm}^2$ at $23\ \mathrm{V}/\mu\mathrm{m}$ for EPAM membranes. The corresponding $U(x,y)$ maps have revealed two initial processing effects as shown in Fig. 7, where two successively measured maps of CNTs on EPAM are compared. Obviously a local emitter current of 10 nA decreases the number density but increases the strength of the remaining emitters. Locally measured $I-V$ curves have confirmed that most of the emitters show current jumps. Only 7% of them on Anodisc® and 15% on EPAM provide stable Fowler–Nordheim (FN) behavior up to about 1 μA, often followed by upward (activation) or downward current jumps (deactivation) up to 2 orders of magnitude (see Fig. 8). Permanent alignment and partial destruction of surface CNTs under high electric fields are the most probable explanations for these processing effects. In rare cases emitter

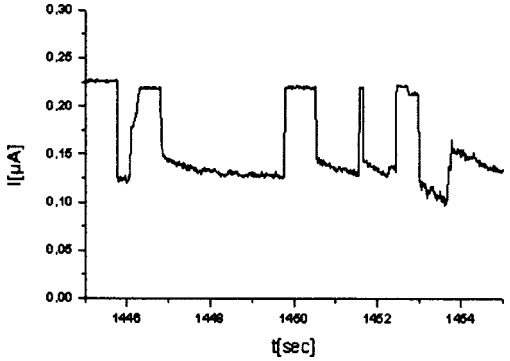

FIG. 9. Short-term current fluctuations of a CNT emitter on Anodisc®. The switching speed (ms) measured with a signal analyzer is limited by the capacity of the FESM.

current saturation with limits up to 12 μA in dc operation was observed. Fast (<ms) reversible switching between current levels was also detected (Fig. 9) which reflect at least bistable emission from different electronic states probably influenced by adsorbates.[15,16]

The stability improvement of the CNT cathodes on EPAM as compared to Anodisc® has been confirmed by long-term current processing in the pressure range between 10^{-6} and 5×10^{-4} mbar. While for CNTs on Anodisc® an initial current of 90 ± 10 μA degraded continuously over 8 h to values between 66% (for 10^{-6} mbar) and 1% (for 5×10^{-4} mbar), on EPAM much less degradation (90% for 2×10^{-6} mbar and 13% for 5×10^{-4} mbar) was achieved (Fig. 10). Accordingly, much better long-term stability was achieved for the latter than for the former ones after current processing up to 700 μA at $6.5\ \mathrm{V}/\mu\mathrm{m}$ for some hours. As result of the processing, in Fig. 11 a current stability of 100 ± 10 μA over 18 h is demonstrated. Therefore, stable CNT emitters on alumina membranes will be available for cold cathode applications.

IV. CONCLUSIONS

The structure of CVD grown CNTs on porous alumina templates depend on their nucleation, the precursors, the

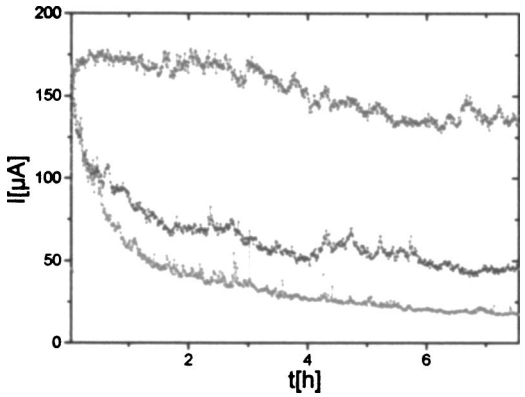

FIG. 10. Long-term current stability ($I_0=150$ μA) of a 28 mm^2 CNT sample on EPAM at various pressures/fields: 2×10^{-6} mbar/4.6 V/μm (upper); 5×10^{-5} mbar/5.3 V/μm (middle); 5×10^{-4} mbar/6.5 V/μm (lower curve).

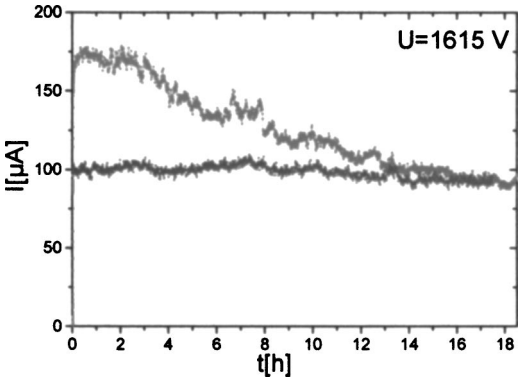

FIG. 11. Comparison of the long-term current stability of the same CNT cathode as in Fig. 10 measured at 10^{-6} mbar and 4.6 V/μm before (upper) and after processing (lower curve) up to 700 μA.

pore diameter and the partial filling of the pores with alumina. We have achieved best field emission results for single ferrocene source grown CNTs on electrochemically etched alumina with 50 nm pores and 200 μm thickness. Separate MWCNTs of about 20 nm diameter and some μm length are fixed to alumina clusters deposited on the surface. Integral FE measurements with luminescent screen on such CNT cathodes have yielded current densities up to 32 mA/cm^2 at 7.2 V/μm based on uniform emitter distributions and number densities of at least 10 000/cm^2. Maximum dc cathode currents up to 10 mA at 900 V were limited by discharges due to phosphor evaporation. Single emitter investigations revealed stable FN-like $I-V$ curves up to 1 μA and saturation currents up to 12 μA. Despite of short-term current fluctuations and emitter activation and destruction effects, the CNT cathodes provided long-term current stability after current processing at pressures up to 5×10^{-4} mbar. Further optimization of these CNT cathodes are underway for diode applications.

ACKNOWLEDGMENTS

The authors thank J. Seekamp at BUW for the SEM measurements. This work was funded in parts by Volkswagen-Stiftung and the Deutsche Forschungsgemeinschaft (DFG), Germany.

[1]J.-M. Bonard, T. Stöckli, O. Noury, and A. Chatelain, Appl. Phys. Lett. **78**, 2775 (2001).
[2]G. Z. Yue, Q. Qiu, B. Gao, Y. Cheng, J. Zhang, H. Shimoda, S. Chang, J. P. Lu, and O. Zhou, Appl. Phys. Lett. **81**, 355 (2002).
[3]K. A. Dean, T. P. Burgin, and B. R. Chalamala, Appl. Phys. Lett. **79**, 1873 (2001).
[4]V. Semet, Vu T. Binh, P. Vincent, D. Guillot, K. B. K. Teo, M. Chhowalla, G. A. J. Amaratunga, W. I. Milne, P. Legagneux, and D. Pribat, Appl. Phys. Lett. **81**, 343 (2002).
[5]L. Nilsson, O. Groening, C. Emmenegger, O. Kuettel, E. Schaller, L. Schlapbach, H. Kind, J.-M. Bonard, and K. Kern, Appl. Phys. Lett. **76**, 2071 (2000).
[6]F. Kaldasch, B. Günther, G. Müller, J. Engstler, and J. J. Schneider, Proceedings 14th International Vacuum Microelectronics Conference, Davis, CA, 2001, IEEE Cat. No. 01TH8586, p. 25.
[7]J.-M. Bonard, K. A. Dean, B. F. Coll, and C. Klinke, Phys. Rev. Lett. **89**, 197602 (2002).
[8]M. Stammler, J. Ristein, T. Habermann, A. Göhl, K. Janischowsky, D. Nau, G. Müller, and L. Ley, Diamond Relat. Mater. **8**, 792 (1999).
[9]Y. Wei, C. Xie, K. A. Dean, and B. F. Coll, Appl. Phys. Lett. **79**, 4527 (2001).
[10]J.-M. Bonard, C. Klinke, K. A. Dean, and B. F. Coll, Phys. Rev. B **67**, 115406 (2003).
[11]K. B. K. Teo, M. Chhowalla, G. A. J. Amaratunga, W. I. Milne, D. Hasko, G. Pirio, P. Legagneux, F. Wyczisk, and D. Pribat, Appl. Phys. Lett. **79**, 1534 (2001).
[12]J. Engstler, dissertation, FB Chemie, University of Duisburg-Essen, Germany, 2003.
[13]B. Günther, dissertation, FB Physik, Berg. University Wuppertal, Germany, 2002.
[14]J. Engstler and D. Lysenkov (unpublished).
[15]R. T. Olsson, G. R. Condon, J. A. Panitz, and P. R. Schwoebel, J. Appl. Phys. **87**, 2031 (1999).
[16]B. Günther, F. Kaldasch, G. Müller, S. Schmitt, T. Henning, R. Huber, and M. Lacher, J. Vac. Sci. Technol. B **21**, 427 (2003).